



# Synthesis and assessment of a graphene-based composite photocatalyst



Pedro Magalhães, Joana Ângelo, Vera M. Sousa, Olga C. Nunes, Luísa Andrade, Adélio Mendes\*

LEPABE – Faculdade de Engenharia, Universidade do Porto, Rua Dr. Roberto Frias, 4200-465 Porto, Portugal

## ARTICLE INFO

### Article history:

Received 2 February 2015

Received in revised form 19 May 2015

Accepted 23 May 2015

Available online 10 June 2015

### Keywords:

P25/graphene

Photoinactivation

Adsorption

Environmental preservation

Global environment

Heterogeneous reaction

## ABSTRACT

A novel composite photocatalyst prepared from graphene and commercial TiO<sub>2</sub> (P25 from Evonik) was synthesized, exhibiting enhanced photocatalytic activity for methylene blue degradation, when compared with pristine P25. Additionally, the new catalyst showed 20% more NO conversion under UV light than P25. The band gap of the catalyst, obtained from diffuse reflectance, was 2.95 eV indicating an extended light absorption up to 420 nm. The novel photocatalyst was further tested for inactivating microorganisms showing better results than the reference photocatalyst. Under visible light, the viability loss of the reference bacterial strain *Escherichia coli* DSM 1103 was two times higher than with the bare P25; it was observed 29% of inactivation with the P25/graphene composite and 14% with the P25 sample, following standard ISO 27447:2009.

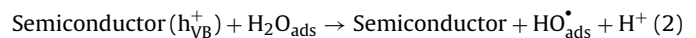
© 2015 Elsevier B.V. All rights reserved.

## 1. Introduction

Photocatalysis has attracted the attention of many researchers mainly because it can be used for photoabatement of atmospheric contaminants, water treatment and inactivation of microorganisms both in suspension and on surfaces [1,2]. More recently, photoinactivation of microorganisms has emerged as an alternative disinfection method [3]; especially the use of titanium dioxide in antimicrobial application has been widely discussed [2,3]. This special interest on TiO<sub>2</sub> material was fueled by the work by Fujishima and Honda [4] in 1972, describing for the first time water splitting using a TiO<sub>2</sub> photoelectrode.

Independently of the photocatalytic application, the mechanism behind photocatalysis consists in the generation of electron–hole pairs upon excitation of the photocatalyst with photons showing energy higher than the band gap (in the case of TiO<sub>2</sub> ca. 3.2 eV) – Eq. (1). These holes and electrons can oxidize and reduce surface-adsorbed molecules, respectively. The strong oxidation potential of the photogenerated valence band holes in anatase TiO<sub>2</sub> ( $E_{VB} = +3.0$  V vs. normal hydrogen electrode (NHE), pH 1) originates the formation of hydroxyl radicals (OH•) when in contact with water – Eq. (2). The reduction potential of anatase TiO<sub>2</sub> conduction band electrons

is of ca.  $-0.2$  V (pH 1) and reduces O<sub>2</sub> to produce superoxide radical (O<sub>2</sub><sup>•−</sup>) – Eq. (3) [5]. These free radicals intermediate the oxidation of organic species at, for example, the surface of microorganisms, originating ultimately their inactivation.



The extensive use of TiO<sub>2</sub> material as photocatalyst can be explained by its thermal and chemical stability, exhibiting no photocorrosion, readily available, relatively cheap and band edges that are well positioned for producing oxidizing/reducing agents [5]. However, TiO<sub>2</sub> absorbs only UV light, preventing its usage under visible spectrum; hence, many efforts have been powered to enhance titanium dioxide photocatalytic activity. Two main actions are being followed: (i) narrowing the semiconductor band gap ( $E_g$ ); and (ii) decrease the  $e^-/h^+$  recombination. While the first allows the photocatalyst to absorb a larger fraction of the solar spectrum and eventually reach the visible spectrum, the later allows improving the redox reactions rate at the photocatalyst surface. Several doping techniques have been described targeting the decrease of the semiconductor band gap [6,7]. Even though the doping mechanism is not yet fully understood, the two most used dopants of TiO<sub>2</sub> are C and N; these dopants act as substitutional anions (sub-

\* Corresponding author.

E-mail address: [mendes@fe.up.pt](mailto:mendes@fe.up.pt) (A. Mendes).

stitute oxygen) or interstitial cations (substitute titanium) [8,9]. On the other hand, to decrease  $e^-/h^+$  recombination rate several studies suggest the use of carbon-based supports such as carbon nanotubes (CNTs), fullerene or graphene [8]. These materials have the ability to receive and store photoinjected electrons and thus preventing  $e^-/h^+$  recombination. In most of the cases, partially oxidized graphene, known as graphene oxide (GO), is used instead of pure graphene due its tunable optical, conductive and chemical properties. Graphene oxide is obtained functionalizing graphene sheets with carboxylic acid, hydroxyl and/or epoxide groups, and thus its properties can be adjusted via chemical modification [10]. The binding of  $\text{TiO}_2$  to graphene sheets allows improved photocatalytic performance when compared with their pristine form mainly because: (i) efficient charge separation and transportation; (ii) extended light absorption range; and (iii) enhanced adsorption [11].  $\text{TiO}_2$ /graphene composites slow the rate of  $e^-/h^+$  recombination after light excitation [12], increasing the charge transfer rate of electrons. The extended light absorption can be achieved due to doping of  $\text{TiO}_2$  with carbon from the graphene, leading to a narrowing of the semiconductor band gap. The enhanced adsorption of the  $\text{TiO}_2$ /graphene composite is mainly attributed to its very large  $\pi$ -conjugation system and two-dimensional planar structure [11,13]. The increase in adsorption may enhance the photocatalytic degradation of methylene blue, assuming the adsorption of reactants is higher than the adsorption of the degradation products. Even though there are some works reporting the use of the  $\text{TiO}_2$ /graphene composites in areas such as dyes degradation evaluation [14] and microorganism photoinactivation [15], the use of  $\text{TiO}_2$ /graphene composites for NO deep oxidation has never been reported in literature.

In this work, a composite photocatalyst was prepared from commercial graphene (xGnP<sup>®</sup> from XG Sciences) and commercial  $\text{TiO}_2$  (P25 from Evonik) and its performance compared with commercial photocatalysts – P25 and VLP7101 (Kronos). The band-gap of the prepared photocatalyst was assessed by diffuse reflectance and it was tested for methylene blue degradation and NO deep oxidation under UV-light. The photocatalyst was further tested for inactivating microorganisms both under UV radiation and visible light. The viability loss of the reference bacterial strain *E. coli* DSM 1103 was obtained for both types of radiation and compared with three commercial photocatalysts: P25, VLP7000 and VLP7101.

## 2. Materials and methods

### 2.1. Synthesis of P25/graphene composite photocatalyst

P25/graphene composite was prepared as described elsewhere [11] with minor modifications. Briefly, oxidized graphene nanoplatelets ( $\text{GNP}_{\text{ox}}$ ) –  $\text{KMnO}_4$  3:1 graphene nano-platelets (GNP) – were prepared according to a modified Hummer's method. Shortly, 50 mL of  $\text{H}_2\text{SO}_4$  were added to 2 g of GNP at room temperature and the solution was cooled using an ice bath, followed by gradual addition of 6 g of  $\text{KMnO}_4$ . Then, 300 mL of distilled water was added, followed by addition of  $\text{H}_2\text{O}_2$  until oxygen release stopped.  $\text{GNP}_{\text{ox}}$  was washed 5 times with water by centrifugation at 4000 rpm during 15 min. The solid was dispersed in 500 mL of water by sonication (Bandelin Sonorex R K512H) during 5 h and lyophilized during 72 h. Then, the composite was obtained via a hydrothermal method based on the work by Zhang et al. [11]. Briefly, 2 mg of  $\text{GNP}_{\text{ox}}$  was dissolved in a solution of distilled  $\text{H}_2\text{O}$  (20 mL) and ethanol (10 mL) by ultrasonic treatment for 1 h, and 0.2 g of P25 was added to the obtained  $\text{GNP}_{\text{ox}}$  solution and stirred for another 2 h to get a homogeneous suspension. The suspension was then placed in a 40 mL Teflon-sealed autoclave and maintained at 120 °C for 3 h to simultaneously achieve the reduction of GO and the deposition of P25 on

the carbon support. Finally, the resulting composite was recovered by filtration, rinsed by deionized water several times and dried at room temperature.

The photocatalytic activity of the as-prepared P25/graphene composite was then compared with three different commercial photocatalysts: Aeroxide<sup>®</sup>  $\text{TiO}_2$  P25 (Evonik Industries, Germany), Kronos<sup>®</sup> VLP7000 and VLP7101 (KRONOS Worldwide, Inc., United States of America).

## 2.2. Characterization

### 2.2.1. Diffuse reflectance analyses

Diffuse reflectance spectroscopy is often used to determine the absorption properties of both crystalline and amorphous materials [16]. The band gap of a sample can be obtained from the Tauc equation, which relates the diffuse reflectance and the Kubelka–Munk model to the excitation frequency [16]:

$$(h\nu F(R_{\infty}))^{1/n} = A (h\nu - E_g) \quad (4)$$

where,  $h$  is the Planck constant,  $\nu$  is the frequency of vibration,  $A$  is a constant and  $E_g$  is the band gap energy.

This equation is obtained multiplying the Kubelka–Munk equation by the energy of the incident radiation ( $E=h\nu$ ) and powered to a coefficient  $n$ , according to the type of the electronic transition of the material. For indirect transitions  $n$  equals 2 and for direct transition  $n$  is 1/2. Plotting the modified Kubelka–Munk equation as a function of the incident radiation, the band gap of the semiconductor can be obtained extrapolating the linear part of this curve to the x-axis, the so-called Tauc plot; the band gap energy is read at the intersection. Diffuse reflectance of the different samples were obtained in a Shimadzu UV-3600 UV-vis-NIR spectrophotometer, equipped with a 150 mm integrating sphere and using  $\text{BaSO}_4$  as 100% reflectance standard. The samples were pressed to form a flat disc that fit into the spectrophotometer sample holder.

### 2.2.2. SEM and XRD analyses

The morphology and composition of the photocatalysts was obtained from scanning electron microscopy (SEM) coupled with energy dispersive X-ray (EDX) analysis. A FEI Quanta 400FEG ESEM/EDAX Genesis X4 M apparatus equipped with a Schottky field emission gun (for optimal spatial resolution) was used for the characterization of the surface morphology of the photocatalysts with SEM. Images were digitally recorded using a Gatan SC 1000 ORIUS CCD camera (Warrendale, PA, USA). These SEM/EDX analyses were made at Centro de Materiais da Universidade do Porto (CEMUP).

The crystallographic characterization of the samples was performed by X-ray diffraction (XRD). The XRD pattern of the selected samples was obtained using a Denchtop X-Ray Diffractometer RIGAKU, model MiniFlex II using Cu X-ray tube (30 KV/15 mA). The data was obtained at  $2\theta$  angles (10–80°), with a step speed of 3.5°/min. Debye–Scherrer equation was used to determine the crystallite size. The obtained X-ray scans were compared to those of standard database and the phases were assigned comparing with data available in literature.

## 2.3. Photoactivity characterization

The photocatalytic performance of the as prepared semiconductors was determined by: (a) degradation of dye methylene blue, (b) nitrogen oxide (NO) deep oxidation and (c) photoinactivation of microorganisms. Each of these techniques is described next.

### 2.3.1. Methylene blue degradation

The photodegradation history of methylene blue (MB) dyes was followed by photospectroscopy. In a typical process, aqueous

Download English Version:

<https://daneshyari.com/en/article/2784>

Download Persian Version:

<https://daneshyari.com/article/2784>

[Daneshyari.com](https://daneshyari.com)